Polyacrylic aerogels for water treatment: Recycle and reuse of metal ions

SHI Wenda, OUYANG Yuxin, WANG Liangbing*
(State Key Laboratory for Powder Metallurgy, School of Materials Science and Engineering, Central South University, Changsha, 410083, China)

Abstract: The adsorption and recovery of metal ions, especially noble metal ions, in aqueous solutions have received increasing attention. Although polyacrylic acid is a promising adsorbent for metal ions, its solubility in water limits its widespread application. This solubility problem can be solved by modifying polyacrylic acid to facilitate the adsorption of metal ions in water. In this study, carbon nanotubes/chitosan/sodium acrylate (CNTs/CS/PAA-Na) aerogels were successfully synthesized as efficient metal adsorbents in aqueous solution. At room temperature, CNTs/CS/PAA-Na exhibited remarkable metal ion adsorption at room temperature with an adsorption capacity of 27.6 mg/g for Cu(II) and 30.4 mg/g for Pd(II). In addition, Cu(II) and Pd(II) absorbed on CNTs/CS/PAA-Na can catalyze the hydrogenation of p-nitrophenol. In this one-step way, the recycle and reuse of noble metal ions have been realized, providing a novel strategy for resource utilization of noble metal ions.

Key words: polyacrylic aerogels; adsorption; noble metal recycling; catalysis application
CIF number: X703; O643.36 **Document Code:** A **Article ID:** 1004-0676(2024)01-0045-11

聚丙烯酸气凝胶在水处理中的应用：金属离子的回收再利用(*英文*)

识文达，欧阳宇欣，王梁炳*
(中南大学 材料科学与工程学院 粉末冶金国家重点实验室，长沙 410083)

摘 要：水溶液中金属离子的回收一直以来都是研究热点，其中贵金属离子的吸附和循环利用广受关注。聚丙烯酸在金属离子吸附中具有广阔前景，但其在水中的易溶解性限制了聚丙烯酸在水溶液中的广泛应用。因此，对聚丙烯酸进行改性解决其水溶性问题，有利于实现聚丙烯酸材料在水溶液中的金属离子吸附。本文成功制备了碳纳米管/壳聚糖/丙烯酸钠(CNTs/CS/PAA-Na)复合气凝胶，以作为水溶液中金属离子的高效吸附剂，在室温下对 Cu(II)和 Pd(II)分别达到 27.6 mg/g 和 30.4 mg/g 的吸附容量。此外，Cu(II)和 Pd(II)被吸附到 CNTs/CS/PAA-Na 上形成的新材料能被应用于催化对硝基苯酚的加氢反应，展现出高效的催化性能。整个过程中，贵金属离子实现了一站式回收和再利用，为贵金属离子资源化利用提供了一种新策略。

关键词：聚丙烯酸气凝胶；吸附；贵金属回收；催化应用

Because of the growing emphasis on water environment management，the recovery of metal ions, including toxic heavy metal ions, noble metal ions, inorganic anions, and organics, has attracted a large amount of attention of researchers[1]. Due to the limited availability of precious metals, to recover them from

收稿日期：2023-02-28
基金项目：中国科协青年人才托举工程(No. YESS20200031)；中南大学科研启动基金(No. 502045005)；浙江新和成股份有限公司产学研合作项目；宁波锋成先进能源材料研究院有限公司产学研合作项目
第一作者：识文达，男，硕士研究生；研究方向：吸附材料；E-mail: swd1150568483@csu.edu.cn
*通信作者：王梁炳，男，教授；研究方向：有色金属光催化；E-mail: wanglb@csu.edu.cn

aqueous and organic solutions is economically attractive[2]. Various efforts, methods such as chemical deposition, ion exchange, filtration, microbial treatment and physical adsorption have been studied to recover heavy metal ions[3-8]. Physical adsorption is a relatively weak adsorption process, which is mainly completed by Van Der Waals force[9-10]. The adsorption process is prompt, and the adsorption equilibrium can be quickly reached, but the adsorption capacity is relatively low. Chemisorption is a strong adsorption process caused by an interface chemical reaction between the adsorbent and the adsorbate, which creats chemical bonds among them[11-14]. Chemisorption has much higher adsorption efficiency than physical adsorption. As a result, grafting functional groups into adsorbents is a more effective and common practice to improve the adsorption performance of materials[15]. As one of most widely used material in the adsorption of water pollutants[16-17], polyacrylic acid (PAA) contains a large number of carboxyl groups that form strong coordinate bonds with metal ions[18]. Furthermore, the carboxyl groups allow PAA to adsorb heavy metals at a variety of conditions via geometric coordinate configuration through the deprotonation process[19-20]. On the other hand, PAA is easily dissolved in water, thus making it difficult to separate PAA and limiting the further application of PAA[21].

Aerogels receive tremendous interests in the adsorption of pollutants due to their low density, free diffusion[22-23], and convenient surface functionalization[24-25]. The aerogels are usually prepared through polymerization reactions of specific molecular precursors, thus providing the possibility to synthesize composite aerogels[26]. The composite aerogels provide desirable combinations of stable composite structure and high exposure of reactive sites, resulting in optimized mechanical properties and enhanced adsorption performance.

Besides the adsorption performance, the subsequent procedure after adsorption is also critical for evaluating the adsorbent practical applications. Acids are commonly used as eluents to achieve metal ion desorption[27]. However, the use of acids may destroy the structure of adsorbent and even pollute the environment[28]. Therefore, it is necessary to develop efficient strategy for reusing adsorbed metal ions.

In this study, we successfully synthesized carbon nanotubes/chitosan/sodium acrylate (CNTs/CS/PAA-Na) composite aerogels as efficient adsorbents. Specifically, the prepared CNTs/CS/PAA-Na aerogels exhibited exceptional adsorption performance in aqueous solution, achieving 27.6 mg/g enrichment capacity for Cu(II) and 30.4 mg/g enrichment capacity for Pd(II) at 20 ℃ and 100 min. Furthermore, the obtained aerogels after adsorption showed outstanding catalytic activity in a hydrogenation reaction. The adsorbed ions were first reduced and employed as active sites, which contributed to the remarkable catalytic activity. The synthesized CNTs/CS/PAA-Na aerogels provide an integrated recycling/application strategy for heavy metals and precious metals ions.

1 Materials and methods

1.1 Chemicals and materials

Chitosan ($(C_6H_{11}NO_4)_n$, 99%), copper chloride dihydrate ($CuCl_2·2H_2O$, 99%), glutaraldehyde ($C_5H_8O_2$, 25%), sodium hydroxide (NaOH, 96%), p-nitrophenol ($C_6H_5NO_3$, 99.5%), sodium borohydride ($NaBH_4$, 98%), potassium persulfate ($K_2S_2O_8$, 99.5%), and potassium sodium tartrate ($C_4H_{12}KNaO_{10}$, 99%) were purchased from Sinopharm Chemical Reagent Co. Ltd. Acrylic acid ($C_3H_4O_2$, 99%), sodium diethyldithiocarbamate ($C_5H_{10}NS_2Na$, 99%), ammonium hydroxide (NH_4OH, 25%), and platinum(IV) chloride ($PtCl_4$, Pt≥57%) were obtained from Shanghai Macklin Biochemical Co. Ltd. Soluble starch ($(C_6H_{10}O_5)_n$, 99%) was purchased from Aladdin Biochemical Technology Co. Ltd. Silver nitrate ($AgNO_3$, 99.8%) was purchased from Xilong Scientific Co. Ltd. Sodium tetrachloropalladate ($Na_2[PdCl_4]$, Pd≥36%) was purchased from Beijing Hwrk Chemical Co. Ltd. Carbon nanotubes (CNTs, 97%) was purchased from Turing Evolution Technology Co. Ltd. in Shenzhen. All chemicals were of analytical grade, used as received, without further purification. All experimental aqueous solutions were prepared with deionized water and its resistivity was 18.2 MΩ·cm.

1.2 Preparation of aerogels

1) Preparation of CS/PAA aerogels. 1 mL of acrylic acid and 30 mg of $K_2S_2O_8$ were first mixed with 5 mL of deionized water in order to synthesize PAA, followed by constantly stirring 0.5 h at 60 ℃. 100 mg of chitosan (CS) was dissolved in 5 mL of 4% acetic acid aqueous solution to form CS solution. PAA was then mixed with 5 mL CS solution, then add 0.4 mL of glutaraldehyde cross-linking agent to obtain CS/PAA hydrogels. Finally, CS/PAA hydrogels were freeze-dried for 24 h to gain CS/PAA aerogels.

2) Preparation of CNTs/CS aerogels. CS solution was first prepared by dissolving 100 mg of CS in 5 mL of 4% acetic acid aqueous solution. 50 mg of carbon nanotubes (CNTs) was mixed with 5 mL of CS solution. Then 0.4 mL of glutaraldehyde cross-linking agent were added into the mixture containing CS and CNTs to form CNTs/CS hydrogels. The CNTs/CS aerogels were obtained after freeze drying for 24 h.

3) Preparation of CNTs/CS/PAA aerogels. 1 mL of acrylic acid, 50 mg of CNTs, and 30 mg of $K_2S_2O_8$ were added into 5 mL of water, followed by heating at 60 ℃ for 0.5 h to form the mixture of PAA and CNTs. CS solution was prepared by dissolving 100 mg of CS in 5 mL of 4% acetic acid aqueous solution. After that, the mixture containing PAA and CNTs was mixed with 5 mL of CS solution, then 0.4 mL of glutaraldehyde was added to crosslink the whole system. The CNTs/CS/PAA aerogels were finally obtained after freeze-drying for 24 h.

4) Preparation of CNTs/CS/PAA-Na aerogels. CS solution was first prepared by dissolving 100 mg of CS in 5 mL of 4% acetic acid aqueous solution. 1 mL of acrylic acid, 50 mg of CNTs, 1 mL of NaOH solution (0.236 $g \cdot mL^{-1}$), and 30 mg of $K_2S_2O_8$ were added into 5 mL deionized water, followed by heating at 60 ℃ for 0.5 h to form CNTs/PAA-Na hydrogels. 5 mL of CS solution was mixed with the CNTs/PAA-Na hydrogels, then added 0.4 mL of glutaraldehyde. After freeze-drying for 24 h, the CNTs/CS/PAA-Na aerogels were obtained.

1.3 Adsorption experiments

The Cu(II) aqueous solutions with different concentrations were prepared by dissolving $CuCl_2 \cdot 2H_2O$ in deionized water. All adsorption performance experiments were performed in 250 mL beakers. In a typical experiment, 450 mg of adsorbent was immersed in 100 mL of Cu(II) aqueous solution (100 ppm) at 20 ℃. After 100 min of reaction, 3 mL of the supernatant was extracted for a spectroscopic measurement. The experiments at other concentrations were the same as the mentioned-above method, except for changing the concentration of Cu(II) ion to 50 ppm, 150 ppm, 200 ppm, and 250 ppm. For pH experiments, the pH value of Cu(II) aqueous solution was defined by dropwise adding either HCl (1 mmol/L) or NaOH (1 mmol/L) solution. The adsorption performance was determined at 30, 40, 50, and 60 ℃. Other experimental conditions were the same as that of the typical procedure. To test the stability of CNTs/CS/PAA-$Cu_{(II)}$ aerogels, the used aerogels were collected and dropped into 1.0 mol/L hydrochloric acid solution to desorb Cu(II), then proceed to the next cycle. In order to measure the adsorption capacity of precious metals, the adsorption tests of CNTs/CS/PAA were conducted in Pd(II), Pt(IV), or Ag(I) ion solutions. The Pd(II), Pt(IV), Ag(I) solutions with concentrations of 100 ppm were prepared by dissolving $Na_2[PdCl_4]$, $PtCl_4$, $AgNO_3$ in deionized water, respectively. The concentrations of precious metal ions were measured by inductively coupled plasma-optical emission spectrometry (ICP-OES).

1.4 Spectroscopic measurement for copper ions

In order to establish the concentration-absorbance standard relationship curve, 1.8 mL of standard Cu(II) solutions with concentrations of 0.2, 0.4, 0.6, 0.8, and 1 ppm were mixed with sodium diethyldithiocarbamate (0.1 mL, 1.0 g/L), sodium potassium tartrate solution (20 μL, 50.0 g/L), starch solution (20 μL, 2.5 g/L), and ammonia solution (0.1 mL, 44.0 g/L). The above mixtures were conducted to the ultraviolet-visible (UV-Vis) absorbance measurement. In order to quantify the adsorption rate of Cu(II), 0.2 mL of the solution after adsorption was diluted to 10 mL. Then 1.8 mL of the diluted solution was taken out to mix with sodium diethyldithiocarbamate (0.1 mL, 1.0 g/L), sodium potassium tartrate solution (20 μL, 50.0 g/L), starch solution (20 μL, 2.5 g/L), and ammonia solution (0.1

mL, 44.0 g/L). The UV-Vis absorbance value of the mixed solution at 435 nm was measured. According to the obtained standard curve, the adsorption value of Cu(II) was obtained from the fitting curve. The adsorption rate equation was shown as follows:

$$\text{Adsorption rate} = (C_0 - C_e)/C_0 \times 100\% \quad (1)$$

where C_0 and C_e represent the initial concentration of Cu(II) and the concentration of Cu(II) after adsorption, respectively.

1.5 Catalytic tests

The CNTs/CS/PAA-Na aerogels were converted into CNTs/CS/PAA-$Cu_{(II)}$ aerogels after absorbing Cu(II). The CNTs/CS/PAA-$Cu_{(II)}$ was firstly reduced with 10 mL $NaBH_4$ (42 mmol/L) to CNTs/CS/PAA-$Cu_{(0)}$, then dried it at 40 ℃ for 2 h under vacuum condition. In a typical hydrogenation of p-nitrophenol reaction, 450 mg CNTs/CS/PAA-$Cu_{(0)}$ was added into the beaker filled with 1 mL of 0.42 mol/L $NaBH_4$ solution, freshly prepared 1 mL of 14 mmol/L p-nitrophenol, and 8 mL deionized water. The catalytic reaction was carried out in a 100 mL beaker with stirring at 20 ℃ for 25 min. 0.2 mL of reaction solution was then diluted to 2 mL to measure the absorbance at 400 nm by UV spectrophotometer. The catalytic performance was carried out at 20, 30, 40, and 50 ℃, and other experimental conditions were similar to the above-mentioned method. To test the stability of CNTs/CS/PAA-$Cu_{(0)}$ aerogels, successive reaction rounds were repeated according to the previous experimental conditions. For the catalytic activity of aerogels after adsorbing precious metal ions, the CNTs/CS/PAA-Na aerogels were converted into CNTs/CS/PAA-$Pd_{(II)}$ aerogels after absorbing Pd(II). The CNTs/CS/PAA- $Pd_{(II)}$ was reduced with 10 mL $NaBH_4$ (42 mmol/L) to CNTs/CS/PAA-$Pd_{(0)}$ and dried it at 40 ℃ for 2 h under vacuum condition. The catalytic experiments of CNTs/CS/PAA-$Pd_{(0)}$ were the same to that of CNTs/CS/PAA-$Cu_{(0)}$.

1.6 Spectroscopic measurement of p-nitrophenol.

The correlation between concentration and absorbance was fitted as a linear standard curve. To determine the p-nitrophenol concentration in the catalyzed reaction, 0.2 mL of the reaction solution was diluted to 2 mL to measure the absorbance value by UV-Vis. The conversion rate of the catalytic reaction was determined by the UV-Vis absorbance value at 400 nm according to the standard curve.

1.7 Instrumentations

The SEM images were recorded on a Quanta FEG 250 scanning electron microscopy. HAADF-STEM images were acquired from a JEOL ARM-200F field-emission transmission electron microscope operating at 200 kV accelerating voltage. XRD patterns were collected by Cu-Kα radiation (λ = 1.54178 Å) from Philips X'Pert Pro Super diffractometer. ICP-OES (Atomscan Advantage, Thermo Jarrell Ash, USA) was used to determine the concentration of metals. XPS measurements were operated in Thermo Fisher Scientific's ESCALAB 250Xi. FT-IR experiments were conducted with a Fourier transform infrared spectrometer (Bruker TENSOR II).

2 Results and discussions

2.1 Synthesis and structural characterizations

The carbon nanotubes/chitosan/sodium acrylate (CNTs/CS/PAA-Na) aerogels were prepared through the copolymerization process as shown in Fig.1. In a typical CNTs/CS/PAA-Na aerogel synthesis, NaOH was first added to the acrylic acid (2:5 molar ratio of NaOH to acrylic acid) to partially neutralize it and form sodium acrylate. Carbon nanotubes and chitosan were subsequently added. After copolymerization and freeze-drying, CNTs/CS/PAA-Na aerogels were finally obtained. Fig.2(a) showed the optical photograph of ultralight CNTs/CS/PAA-Na aerogel. The obtained CNTs/CS/PAA-Na aerogels were ultralight with the density of 2.5 mg/cm^3 and could easily stand on the top of dandelion floating seeds. SEM images of the CNTs/CS/PAA-Na were shown in Fig.2(b) and Fig.2(c), where a three-dimensional morphology with cross-linked network was clearly observed. X-ray photoelectron spectroscopy (XPS) measurements were carried out to characterize the electronic property of CNTs/CS/PAA-Na. Fig.3(a) displayed the C 1*s* XPS spectrum, the main component centered at 284.8 eV which belongs to C-H band, whereas the peaks at 286.3 and 288.8 eV were indexed to C-O and O-C=O, respectively [29-30].

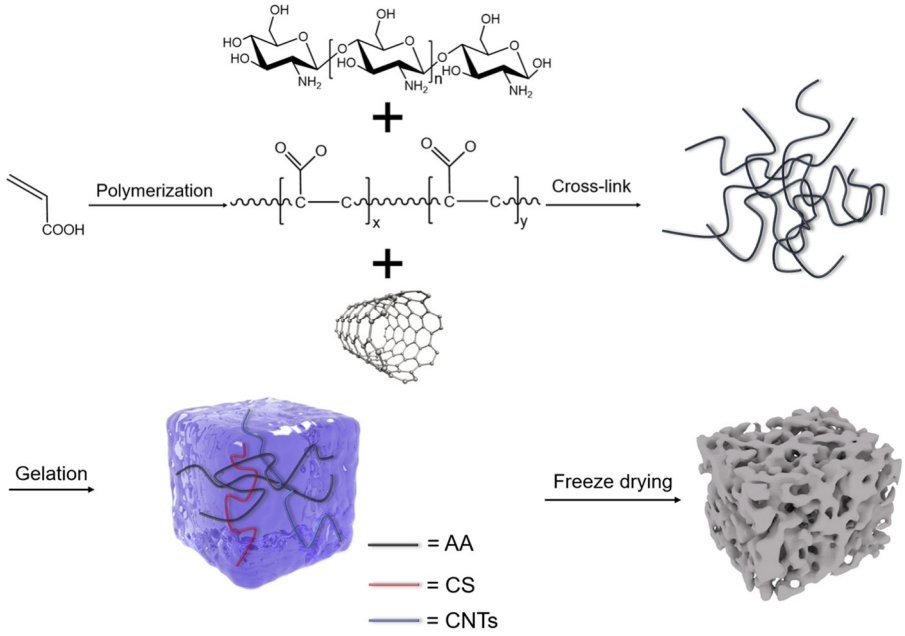

Fig.1 Schematic illustration of the synthetic procedure for CNTs/CS/PAA-Na aerogels

图 1 CNTs/CS/PAA-Na 气凝胶的合成过程示意图

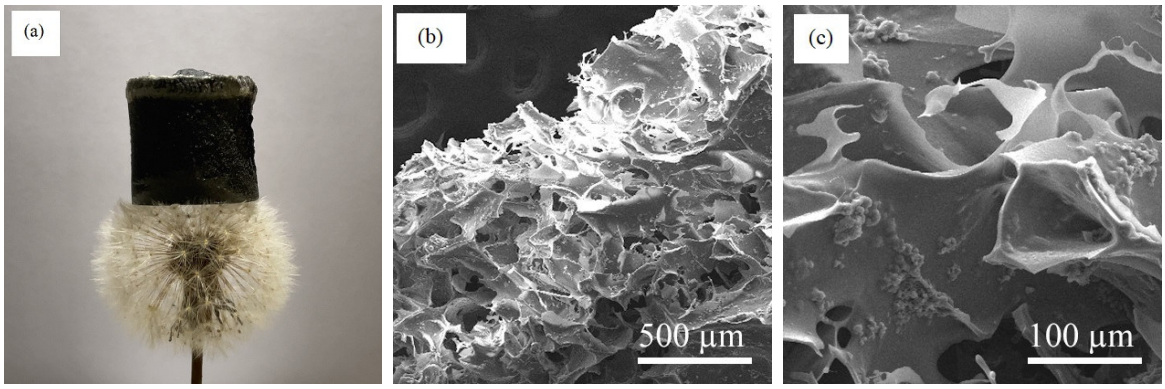

(a). Photograph(实物图); (b). SEM image(SEM 图像); (c). Magnified SEM images (高倍 SEM 图像)

Fig.2 Image of CNTs/CS/PAA-Na aerogels

图 2 CNTs/CS/PAA-Na 气凝胶的图像

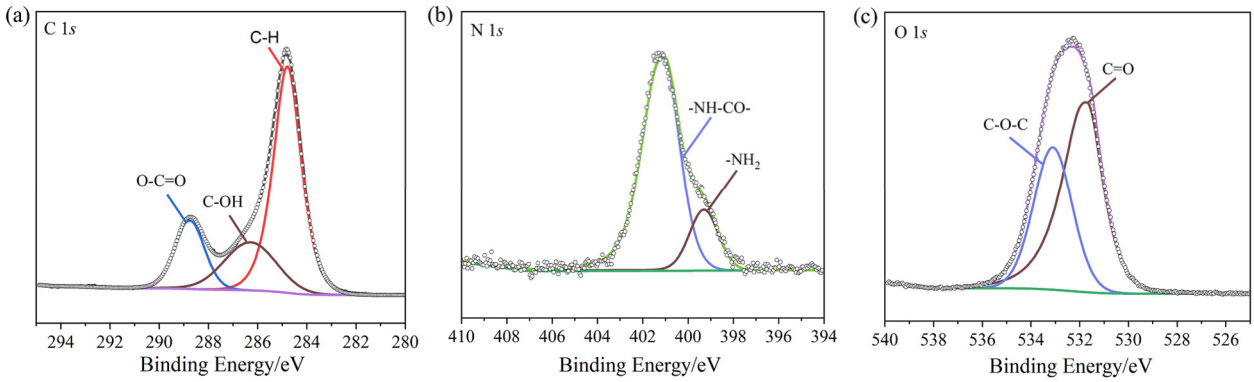

(a). C 1*s* XPS spectrum, (b). N 1*s* XPS spectrum; (c). O 1*s*

Fig.3 XPS spectra of CNTs/CS/PAA-Na aerogels

图 3 CNTs/CS/PAA-Na 气凝胶的 X 射线光电子能谱(XPS)

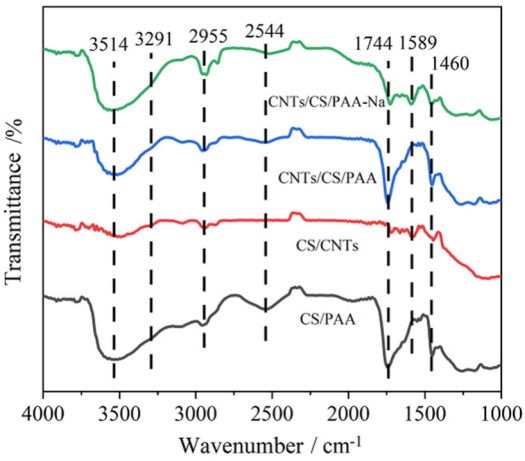

Fig.4 FTIR spectra of as-obtained aerogels

图 4 样品的傅里叶红外光谱

As shown in Fig.3(b), the N 1*s* XPS spectrum of CNTs/CS/PAA-Na was fitted with two peaks [31], corresponding to -NH_2 at 399.3 eV and -NH-CO- at 401.1 eV. As for O 1*s* XPS spectra [30], two peaks at 531.7 and 533.1 eV were assigned to C=O and C-O-C, respectively as shown in Fig.3(c). In addition to CNTs/CS/PAA-Na, CNTs/CS/PAA, CS/CNTs, and CS/PAA aerogels were also prepared by copolymerization and freeze-drying processes using various precursors. Besides, the Fourier-transform infrared (FTIR) were also use to confirm those chemical bonds (Fig.4). With the introduction of the PAA, two peaks appeared at 2544 and 1744 cm^{-1} were corresponded to -OH bending vibration and the C=O stretching vibration. In addition, the peaks at 3514, 3291, 2955, 1589, and 1460 cm^{-1} were indexed to -NH_2, -OH, -CH_2, -HN-, and -CH_3, respectively. The results of FTIR were consistent with the results of XPS.

2.2 Adsorption experiments

The adsorption properties of the as-obtained aerogels were studied. Each experiment was carried out in a 250 mL beaker containing 450 mg of aerogels and 100 mL of 100 ppm Cu(II) aqueous solution at 20 ℃ for 100 min's adsorption. In a typical experiment, kept pH=7. The concentration of Cu(II) aqueous solution was determined by spectroscopic method.

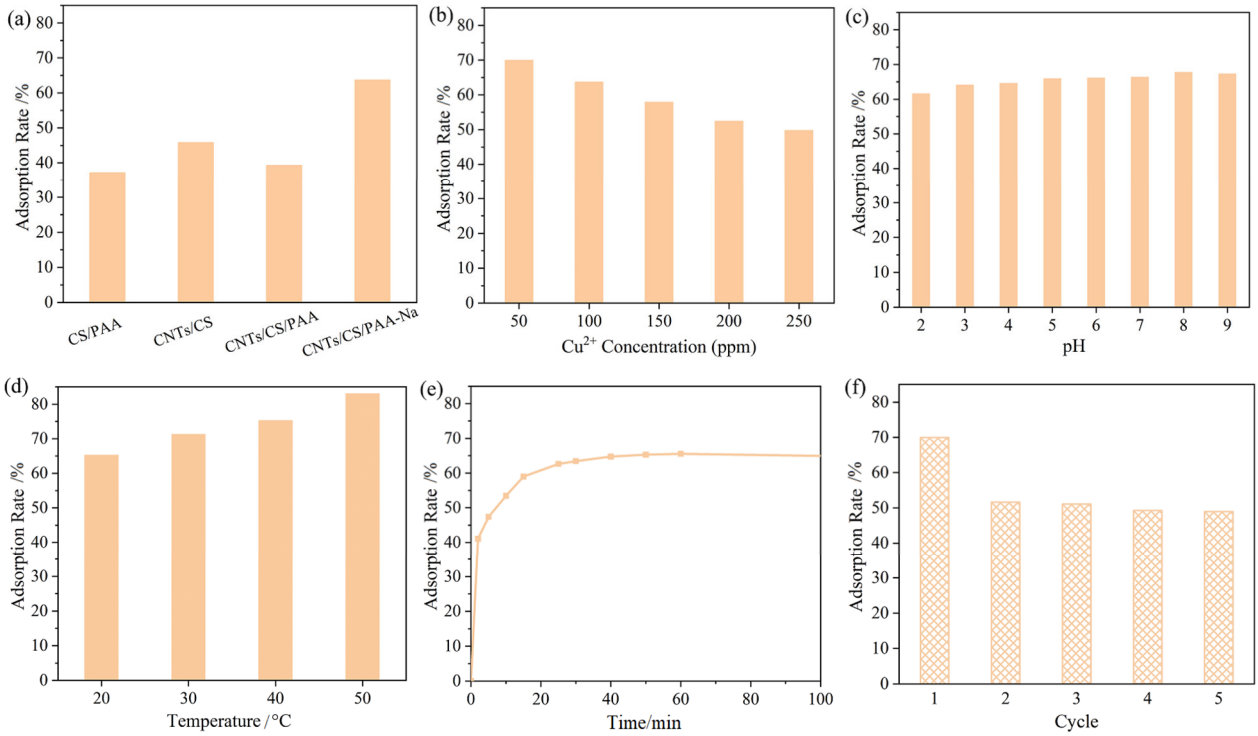

(a). Different aerogels (不同气凝胶); (b). Different Cu(II) concentrations (不同 Cu(II)浓度); (c). Different pH values (不同 pH 值); (d). Different temperatures (不同温度); (e). The dynamic adsorption curve (动态吸附曲线); (f). Cyclic tests (循环吸附)

Fig.5 Adsorption properties of as-obtained CNTs/CS/PAA-Na aerogel in Cu(II) solution (ρ($Cu_{(II)}$)=100 ppm, 20 ℃, 100 min)

图 5 CNTs/CS/PAA-Na 气凝胶对铜离子水溶液的吸附性能(ρ($Cu_{(II)}$)=100 ppm, 20 ℃, 100 min)

Fig.5(a) showed that 63.7% of Cu(II) was adsorbed to CNTs/CS/PAA-Na, and 37.2%, 45.8% and 39.3% of Cu(II) was adsorbed to CS/PAA, CNTs/CS, and CNTs/CS/PAA, respectively. Besides, the adsorption properties of aerogels at different Cu(II) concentrations were also researched. As illustrated in Fig.5(b), the adsorption rate of CNTs/CS/PAA-Na reached up to 70.0% in 50 ppm Cu(II) solution. The adsorption rate was decreased from 69.96% to 49.74% with increase of Cu(II) concentration from 50 ppm to 250 ppm. But the adsorbing capacity of Cu(II) was increased from 7.77 mg/g to 27.63 mg/g when the Cu(II) concentration was increased to 250 ppm. The adsorption capacity of CNTs/CS/PAA-Na reached 27.6 mg/g in 250 ppm Cu(II) aqueous solution. Furthermore, it was worth noting that pH value also had an effect on adsorption performance. Fig.5(c) displayed the adsorption efficiency of CNTs/CS/PAA-Na in 100 ppm Cu(II) aqueous solution at different pH values. When the pH value of the solution increased from 2 to 9, the adsorption rate of Cu(II) was promoted from 61.6% to 67.8%. Moreover, the effect of temperature on the adsorption performance were investigated at at various temperatures. Fig.5(d) showed that the removal efficiency was increased with temperature. The adsorption rate was up to 83.2% at 50°C. Fig.5(e) showed the absorption curve of Cu(II) adsorption on CNTs/CS/PAA-Na. The adsorption of Cu(II) increased with time within 50 min and then reached a stable value of 65.6%. In order to test the stability of CNTs/CS/PAA-Na, successive reaction rounds were performed (Fig.5(f)). After one round, the CNTs/CS/PAA-Na aerogel was added into 1.0 mol/L hydrochloric acid solution to desorb Cu(II). After four rounds, the adsorption rate was 51.6%. In addition, the adsorption performance of CNTs/CS/PAA-Na aerogels to precious metals were investigated. The concentrations of precious metal ions were measured by ICP-OES. The stable adsorption rates of Pd(II), Pt(IV), and Ag(I) were 77.2%, 58%, and 52.8%, respectively.

After Cu(II) was adsorbed to CNTs/CS/PAA-Na aerogels, resulting innew aerogels, CNTs/CS/PAA-$Cu_{(II)}$ aerogels. High-angle-annular-dark-field scanning transmission electron microscopy (HAADF-STEM) and corresponding energy dispersive X-ray (EDX) elemental-mapping energy spectrum were used to verify the adsorption of Cu(II). As displayed in Fig.6, CNTs and CS constituted the self-supporting skeletons structure for the copolymer aerogels and chitosan and sodium acrylate were wrapped around carbon nanotubes. The EDX elemental mapping images of CNTs/CS/PAA-$Cu_{(II)}$ aerogels demonstrated the homogeneous distribution of C, N, O, and Cu elements, indicating the uniform adsorption of Cu(II) (Fig.6). The electronic property of CNTs/CS/PAA-$Cu_{(II)}$ aerogels was also studied. The C 1*s*, N 1*s*, and O 1*s* XPS signals of CNTs/CS/PAA-$Cu_{(II)}$ were the same as the signal of CNTs/CS/PAA-Na, the XPS characteristic peak signals were not affect by adsorption behavior, confirming the CNTs/CS/PAA-Na aerogels kept the original state (Fig.7). Besides, the self-supporting characteristics of CNTs/CS/PAA-Na aerogels assisted to maintain their stability. As shown in Fig.7, two peaks were fitted into $2p_{3/2}$ at 933.5 eV and Cu $2p_{1/2}$ at 953.27 eV, representing the existence of Cu(II). Therefore, CNTs/CS/PAA-Na aerogels were able to efficiently and uniformly adsorb Cu(II) in aqueous solution.

2.3 Catalytic performance tests

The hydrogenation reaction of p-nitrophenol was chosen to evaluate the catalytic activity of synthesized areogels. Before the catalytic hydrogenation reaction test, the CNTs/CS/PAA-$Cu_{(II)}$ was reduced to CNTs/CS/PAA-$Cu_{(0)}$ by using $NaBH_4$ aqueous solution. The hydrogenation reaction was carried out in a 100 mL beaker containing 450 mg aerogels, 1 mL p-nitrophenol aqueous solution (14 mmol/L), 1 mL freshly prepared $NaBH_4$ aqueous solution (0.42 mol/L) and 8 mL deionized water. The specific reaction is as follows:

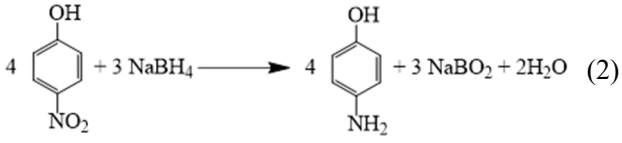

(2)

The concentration of yellow p-nitrophenol solution was proportional to its absorbance at 400 nm, while the p-aminophenol product was colorless. Therefore, the conversion rate of p-nitrophenol was able to be qualified by measuring its absorption at 400 nm. The solution system without catalyst had no color

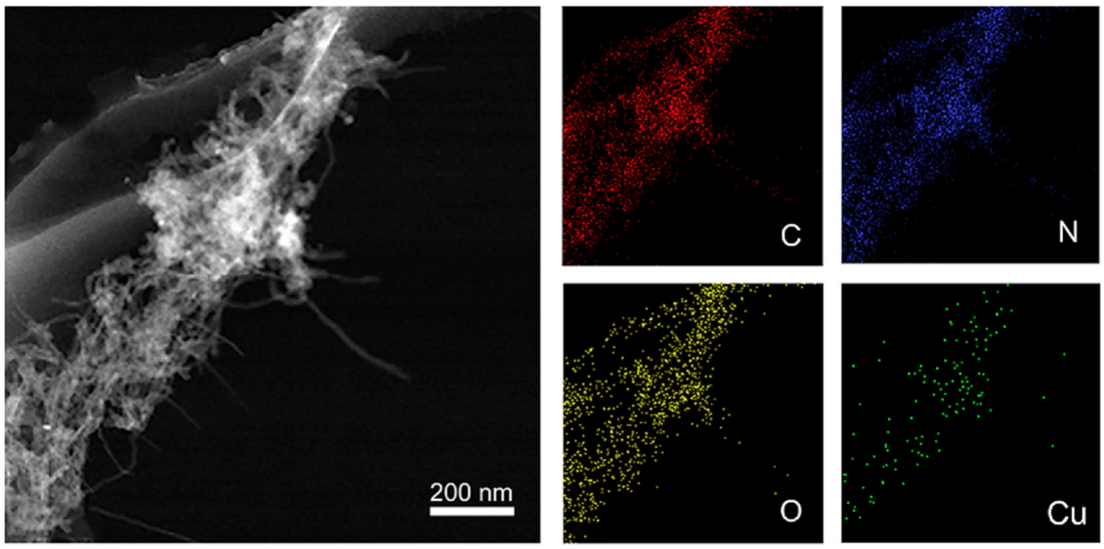

Fig.6 HAADF-STEM images and corresponding EDX elemental mapping images

图 6 CNTs/CS/PAA-$Cu_{(II)}$气凝胶的 HAADF-STEM 图像及其对应的 EDX 能谱图像

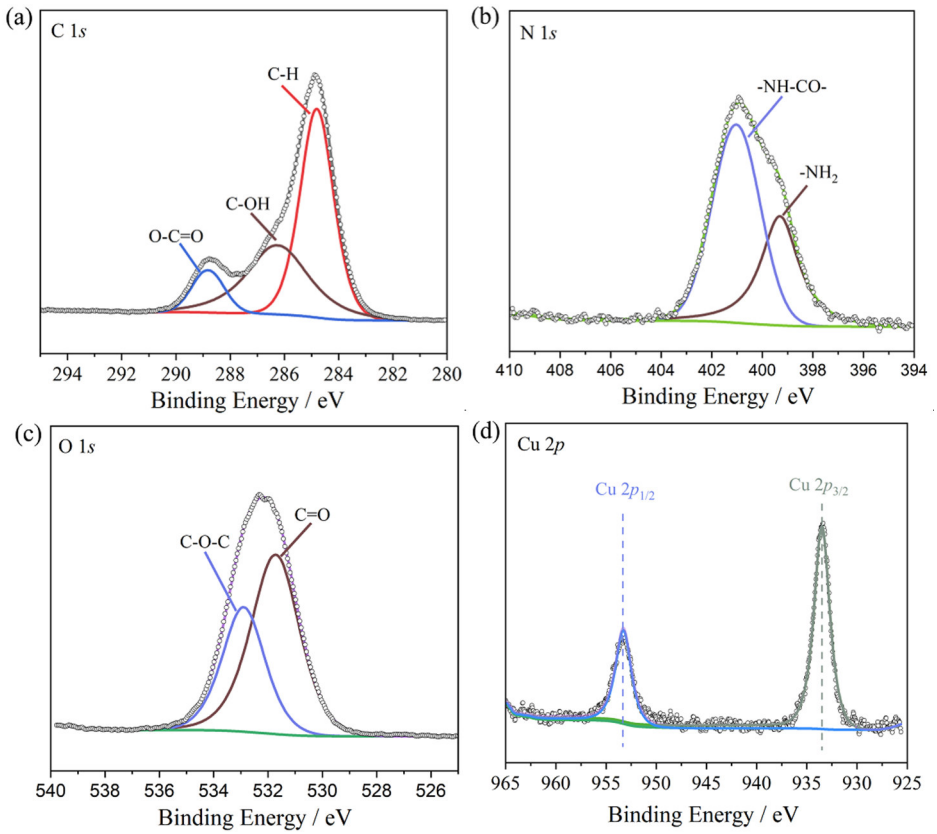

(a). C 1s; (b). N 1*s*; (c). O 1*s*; (d) Cu 2*p*

Fig.7 XPS spectra of CNTs/CS/PAA-$Cu_{(II)}$ aerogels.

Fig.7 CNTs/CS/PAA-$Cu_{(II)}$气凝胶的 X 射线光电子能谱

change and remained stable within 25 minutes which can be used as blank control check. With the introduction of aerogels as catalysts, the dynamic curves of the p-nitrophenol conversion curve were obtained. The catalytic hydrogenation reaction rate increased with temperature, and the conversion rate of p-nitrophenol reached up to 98.1% after 25 min at 20, 30, 40 and 50 ℃. The reaction kinetics was also

studied. The concentration of $NaBH_4$ greatly exceeds the concentration of p-nitrophenol, implying that the concentration of $NaBH_4$ remains constant throughout the reaction. It can also be calculated the profiles of ln (C_t/C_0) *versus* time, where C_t and C_0 represented distinct and the initial concentrations of p-nitrophenol, respectively. The reaction is controlled by a pseudo-first-order kinetics according to the linear relationship between ln (C_t/C_0) and time. The calculated reaction rate constants (k) were 5.33×10^{-2}, 9.185×10^{-2}, 0.106 and 0.132 min^{-1} for the CNTs/CS/PAA-$Cu_{(0)}$ catalyst at 20, 30, 40 and 50 ℃, respectively. It can be conclued a linear fitting line of ln k versus $1/T$ according to the Arrhenius equation (3):

$$\ln k = \ln A - E_a/RT \quad (3)$$

The calculated activation energy (E_a) for CNTs/CS/PAA-$Cu_{(0)}$ was 42.58 kJ/mol. In addition, in order to evaluate the stability of the catalytic performance, continuous reaction tests were carried out. It can be confirmed from the cycle test that the catalytic efficiency of CNTs/CS/PAA-$Cu_{(0)}$ aerogel was more than 95% after four repeated tests, demonstrating the excellent catalytic stability.

The CNTs/CS/PAA-$Pd_{(II)}$ aerogels were also used to catalyze the hydrogenation reaction of p-nitrophenol. After the CNTs/CS/PAA-$Pd_{(II)}$ was treated with $NaBH_4$ solution, Pd(II) was reduced to Pd(0) and the aerogel existed as CNTs/CS/PAA-$Pd_{(0)}$. As shown in Fig.8(a), the conversion rate of p-nitrophenol reached 95.6% after 30 min at 20 ℃, and the reaction rate increased with temperature. Fig.8(b) displayed the linear profiles of ln(C_t/C_0) *versus* time. The calculated reaction rate constants (k) were 7.19×10^{-2}, 8.42×10^{-2}, 10.73×10^{-2}, and 13.91×10^{-2} min^{-1} at 20, 30, 40 and 50 ℃, respectively. The Arrhenius curve was fitted in Fig.8(c), where the activation energy (E_a) for CNTs/CS/PAA-$Pd_{(0)}$ was 39.76 kJ/mol. Furthermore, CNTs/CS/PAA-$Pd_{(0)}$ showed excellent recyclability, and it still has 93.5% of the initial catalytic efficiency after successive reaction rounds as shown in Fig.8(d).

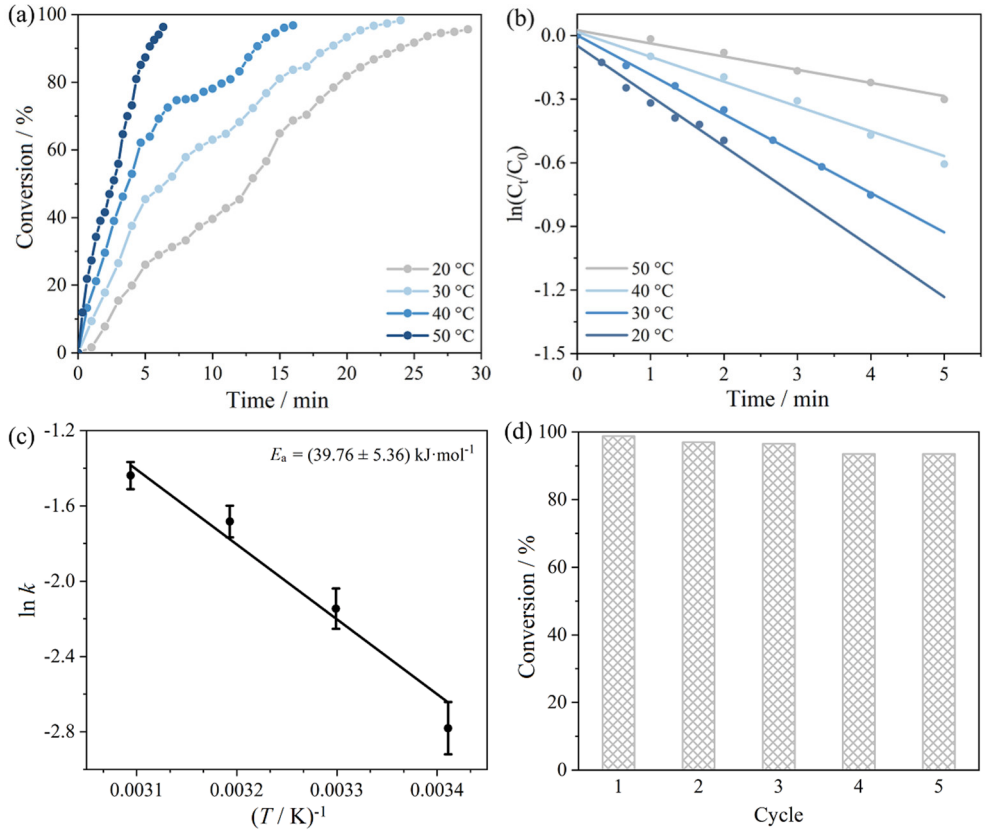

(a). Different temperatures (不同温度); (b). The plots of ln (C_t/C_0) versus time at different temperatures (不同温度下 ln (C_t/C_0)随时间的变化曲线); (c). The Arrhenius plots (阿仑尼乌兹曲线); (d). Catalytic cycle tests of (催化循环测试)

Fig.8 The catalytic hydrogenation performance of p-nitrophenol conversion over CNTs/CS/PAA-$Pd_{(0)}$ aerogels

图 8 CNTs/CS/PAA-$Pd_{(0)}$气凝胶的对硝基苯酚加氢催化性能

3 Conclusion

The CNTs/CS/PAA-Na aerogels were successfully synthesized as efficient adsorbents of metal ions. The prepared CNTs/CS/PAA-Na aerogels exhibited 70.0% adsorption rate for Cu(II) ions and 77.2% adsorption rate of Pd(II) ions at 20 ℃ during 100 min. Moreover, the CNTs/CS/PAA-Na adsorbed Cu(II) and Pd(II) can catalyze the hydrogenation reaction. CNTs/CS/PAA-$Cu_{(0)}$ and CNTs/CS/PAA-$Pd_{(0)}$ showed outstanding activity in the catalytic hydrogenation reaction of p-nitrophenol. This work presents a notably effective CNTs/CS/PAA-Na adsorbent for recycling metal ions in water by enrichment. Furthermore, it paves the way for a new route to adsorption and catalysis, realizing the reuse of noble metal resources.

References:

[1] HOKKANEN S, BHATNAGAR A, SILLANPÄÄ M. A review on modification methods to cellulose-based adsorbents to improve adsorption capacity[J]. Water Research, 2016, 91: 156-173.

[2] DAS N. Recovery of precious metals through biosorption - A review[J]. Hydrometallurgy, 2010, 103: 180-189.

[3] NAMASIVAYAM C, RANGANATHAN K. Removal of Pb(II), Cd (II), Ni (II) and mixture of metal ions by adsorption onto 'waste' Fe (III)/Cr (III) hydroxide and fixed bed studies[J]. Environmental Technology, 1995, 16(9): 851-860.

[4] MUKHERJEE R, BHUNIA P, DE S. Impact of graphene oxide on removal of heavy metals using mixed matrix membrane[J]. Chemical Engineering Journal, 2016, 292: 284-297.

[5] FU F, WANG Q. Removal of heavy metal ions from waste waters: A review[J]. Journal of Environmental Management, 2011, 92(3): 407-418.

[6] ALYÜZ B, VELI S. Kinetics and equilibrium studies for the removal of nickel and zinc from aqueous solutions by ion exchange resins[J]. Journal of Hazardous Materials, 2009, 167: 482-488.

[7] JAMALY S, DARWISH N N, AHMED I, et al. A short review on reverse osmosis pretreatment technologies[J]. Desalination, 2014, 354: 30-38.

[8] MARQUES P, ROSA M, PINHEIRO H. pH effects on the removal of Cu^{2+}, Cd^{2+} and Pb^{2+} from aqueous solution by waste brewery biomass[J]. Bioprocess Engineering, 2000, 23(2): 135-141.

[9] LIU S, LIU J, LIU X, et al. Non-classical hydrogen storage mechanisms other than chemisorption and physisorption[J]. Applied Physics Reviews, 2022, 9(2): 021315.

[10] HUBER F, BERWANGER J, POLESYA S, et al. Chemical bond formation showing a transition from physisorption to chemisorption[J]. Science, 2019, 366(6462): 235-238.

[11] WANG L, SHI C, PAN L, et al. Rational design, synthesis, adsorption principles and applications of metal oxide adsorbents: A review[J]. Nanoscale, 2020, 12(8): 4790-4815.

[12] RICHEY N E, DE PAULA C, BENT S F. Understanding chemical and physical mechanisms in atomic layer deposition[J]. The Journal of Chemical Physics, 2020, 152(4): 040902.

[13] JIANG H, YANG Y, LIN Z, et al. Preparation of a novel bio-adsorbent of sodium alginate grafted polyacrylamide/graphene oxide hydrogel for the adsorption of heavy metal ion[J]. Science of the Total Environment, 2020, 744: 140653.

[14] SIMS R A, HARMER S L, QUINTON J S. The role of physisorption and chemisorption in the oscillatory adsorption of organosilanes on aluminium oxide[J]. Polymers, 2019, 11(3): 410.

[15] ZHU Q, WANG X, CHEN D, et al. Highly porous carbon xerogels doped with cuprous chloride for effective CO adsorption[J]. ACS Omega, 2019, 4: 6138-6143.

[16] DIDEHBAN K H, MOHAMMADI L, AZIMVAND J. Preparation of RGO/Fe_3O_4/poly(acrylic acid) hydrogel nanocomposites with improved magnetic, thermal and electrochemical properties[J]. Materials Chemistry and Physics, 2017, 195: 162-169.

[17] HE J, SUN F, HAN F, et al. Preparation of a novel polyacrylic acid and chitosan interpenetrating network hydrogel for removal of U(VI) from aqueous solutions[J]. RSC Advances, 2018, 8(23): 12684-12691.

[18] FENG E, LI J, ZHENG G, et al. Mechanically toughened conductive hydrogels with shape memory behavior toward self-healable, multi-environmental tolerant and bidirectional sensors[J]. Chemical Engineering Journal, 2022, 432: 134406.

[19] LI X, CAO R, BI W, et al. A new family of cadmium(II) coordination polymers from coligands: Efect of the coexistent groups (R= H, -NO_2, -OH) on crystal structures

and properties[J]. Crystal Growth & Design, 2005, 5(4): 1651-1656.

[20] GODLEWSKA-ŻYŁKIEWICZ B, ŚWISŁOCKA R, KALINOWSKA M, et al. Biologically active compounds of plants: Structure-related antioxidant, microbiological and cytotoxic activity of selected carboxylic acids[J]. Materials, 2020, 13(19): 4454.

[21] ZHAO C, DOLMANS L, ZHU X X. Thermoresponsive behavior of poly(acrylic acid-co-acrylonitrile) with a UCST [J]. Macromolecules, 2019, 52(12): 4441-4446.

[22] ARABKHANI P, ASFARAM A. Development of a novel three-dimensional magnetic polymer aerogel as an efficient adsorbent for malachite green removal[J]. Journal of Hazardous Materials, 2020, 384: 121394.

[23] FRICKE J, TILLOTSON T. Aerogels: Poduction, characterization, and applications[J]. Thin Solid Films, 1997, 297(1): 2122-23.

[24] PIGNATARO B, LICCIARDELLO A, CATALDO S, et al. SPM and TOF-SIMS investigation of the physical and chemical modification induced by tip writing of self-assembled monolayers[J]. Materials Science and Engineering C, 2003, 23(1): 7-12.

[25] KESHAVARZ L, GHAANI M R, MACELROY J M D, et al. A comprehensive review on the application of aerogels in CO_2-adsorption: Materials and characterisation[J]. Chemical Engineering Journal, 2021, 412: 128604.

[26] CAI B, EYCHMüLLER A. Promoting electrocatalysis upon aerogels[J]. Advanced Materials, 2019, 31: 1804881.

[27] GAO C, WANG X L, AN Q D, et al. Synergistic preparation of modified alginate aerogel with melamine/ chitosan for efficiently selective adsorption of lead ions[J]. Carbohydrate Polymers, 2021, 256: 117564.

[28] FAN S, CHEN J, FAN C, et al. Fabrication of a CO_2-responsive chitosan aerogel as an effective adsorbent for the adsorption and desorption of heavy metal ions[J]. Journal of Hazardous Materials, 2021, 416: 126225.

[29] LOUETTE P, BODINO F, PIREAUX J J. Poly(acrylic acid) (PAA) XPS reference core level and energy loss spectra[J]. Surface Science Spectra, 2005, 12(1): 22-26.

[30] LI J, HOU X, MAO Y, et al. Enhanced performance of aprotic electrolyte LiO_2 batteries with SnS_2-SnO_2/C heterostructure as efficient cathode catalyst[J]. Energy & Fuels, 2020, 34(11): 14995-5003.

[31] KATAN T, KARGL R, MOHAN T, et al. Solid phase peptide synthesis on chitosan thin films[J]. Biomacromolecules, 2022, 23(3): 731-742.

＊＊

《贵金属》入编《中文核心期刊要目总览》2023 年版

2023 年年底，收到北京大学图书馆、《中文核心期刊要目总览》2023 年版编委会通知（入编通知见本期封 3）：

“依据文献计量学的原理和方法，经研究人员对相关文献的检索、统计和分析，以及学科专家评审，《贵金属》入编《中文核心期刊要目总览》2023 年版（即第 10 版）之“冶金工业”类的核心期刊。”

自 1992 年以来，《贵金属》已多次入编《中文核心期刊要目总览》，包括：

1992 年（第 1 版）、1996 年（第 2 版）、2008 年（第 5 版）、2011 年（第 6 版）、2014 年（第 7 版）、2017 年（第 8 版）、2010 年（第 9 版）、2023 年（第 10 版）。

本刊将秉持办刊宗旨，为作者和读者提供更好的服务，为贵金属学科发展做出积极的贡献。

《贵金属》编辑部

2024 年 3 月